Progress In Electromagnetics Research Letters, Vol. 102, 57–65, 2022

Linearly Polarized and Circularly Polarized Cylindrical Dielectric Resonator Antenna

Lakshminarayana Usha[1, *] and Kandasamy Krishnamoorthy[2]

Abstract—This paper presents the design of a novel aperture coupled cylindrical dielectric resonator antenna with linear polarization and circular polarization. The linearly polarized cylindrical dielectric resonator antenna (LP CDRA) with proposed aperture and microstrip feed line excites three hybrid radiating modes ($HEM_{11\delta}$, $HEM_{21\delta}$, and $HEM_{13\delta}$) in three impedance bands. The circularly polarized cylindrical dielectric resonator antenna (CP CDRA) with proposed aperture and flag-shaped feed line excites six different hybrid radiation modes ($HEM_{11\delta}$, $HEM_{21\delta\text{-like}}$, $HEM_{21\delta}$, $HEM_{12\delta}$, $HEM_{13\delta}$, $HEM_{14\delta}$) in three impedance bands and three CP bands. A different sense of CP is reported. The antennas operate in both C and X bands.

1. INTRODUCTION

Cylindrical dielectric resonator antenna (CDRA) has gained much attention for its design flexibility and hybrid radiating modes [1–5]. Higher-order modes have high gain and very good broadside radiation characteristics. In [2–6], authors have suggested many new techniques for higher-order hybrid mode excitation in CDRA with a different feeding mechanism. In [4] and [5], a new composite aperture is used to excite two and quad hybrid modes, respectively. In [6], twin aperture is used to excite $HEM_{11\delta}$ and $HEM_{11\delta+1}$ with suppressed $HEM_{21\delta}$ modes. It is often challenging to excite hybrid radiating modes and their higher-order modes simultaneously. Our proposed linearly polarized cylindrical dielectric resonator antenna (LP CDRA) with non-resonant "triangular aperture" demonstrates the excitation of $HEM_{21\delta}$ along with $HEM_{11\delta}$ and higher-order $HEM_{13\delta}$ modes at different frequencies simultaneously. The LP CDRA provides resonances at 4.36, 6.56, and 8.89 GHz with impedance bandwidths of 6.62%, 6.87%, and 9.55% and gains of 5.7 dBi, 3.9 dBi, and 8.2 dBi, respectively. The LP CDRA design concept is presented in Section 2.

Circularly polarized (CP) dielectric resonator antennas (DRA) are desirable in satellite and modern wireless communication to overcome multipath and alignment problems. Multiband antennas are widely required in the recent era of wireless communication for different frequency band applications simultaneously. Modern wireless communication requires multi-CP band DRAs. In [3, 7], multiband and triband are obtained in CDRA using composite feeding. Dual-band CP is generated by introducing notches [8], truncating opposite corners of the DRA [9], and a metallic strip with an inverted-sigmoid shape [10]. Several dual-band, triple-band CP DRAs have been reported with different structures and feeding techniques. Most of them are designed with complex DRA geometries and feed. This work also proposes a standard CDRA with simplified feed to achieve circular polarization with a triangular aperture and flag shape feed. The proposed CP CDRA is triband with six different hybrid radiating modes and three CP bands. The CP CDRA provides three impedance bands with percentage bandwidths of 13.02% (4.39–4.99 GHz), 17.9% (5.92–7.12 GHz), and 19.51% (8.05–9.79 GHz), and three

Received 23 November 2021, Accepted 6 January 2022, Scheduled 10 January 2022

* Corresponding author: Lakshminarayana Usha (lusharamesh@gmail.com).

[1] National Institute of Technology, Surathkal, Mangalore, Karnataka, India. [2] Department of Electronics and Communication, National Institute of Technology, Surathkal, Mangalore, Karnataka, India.

CP bands with axial ratio bandwidths of 1.39%, 1.21%, and 0.31% having center frequencies 8.6, 9.1, and 9.6 GHz. The CP CDRA design concept is presented in Section 3. Section 4 gives the conclusion.

2. LINEARLY POLARIZED CYLINDRICAL DIELECTRIC RESONATOR ANTENNA

2.1. Physical Insight of the Antenna Structure

Figure 1 shows the configuration of realized triband LP CDRA. Roger's TMM10i has a permittivity $\epsilon_r = 9.8$, loss tangent 0.0022, radius 10 mm, and height 6.35 mm. The CDRA is mounted at the center of the ground plane of size 50 mm × 50 mm. The CDRA is supported with a substrate FR-4 with permittivity $\epsilon_s = 4.3$, height $h_s = 0.8$ mm, and $\tan\delta = 0.0025$. The bottom side of the substrate is printed with a microstrip feed line of width w_s and length l_f. The CDRA is excited by an equilateral triangular slot at the center on the ground of sides 10.39 mm.

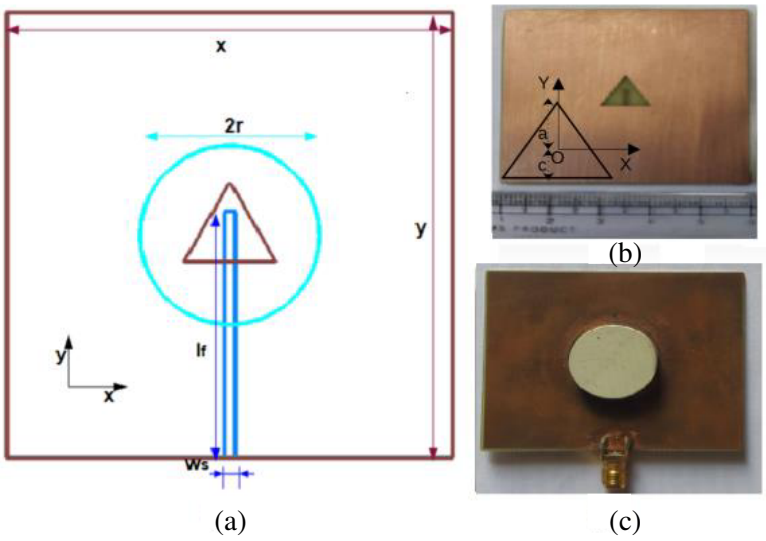

Figure 1. (a) Top view of all the layers of the proposed triband LP CDRA. Fabricated prototype of the proposed triband LP CDRA, (b) triangular slot on the ground plane and (c) top view. $x = 50$, $y = 50$, $r = 10$, $w_s = 1.2$ and $l_f = 31.48$ (all dimensions are in mm).

The aperture coupling produces $HEM_{11\delta}$ and its higher-order modes inside CDRA. The aperture acts as a magnetic dipole, so $HEM_{11\delta}$ and $HEM_{13\delta}$ modes are produced in CDRA. The triangular aperture improves the coupling to resonant $HEM_{11\delta}$ along with the other two hybrid modes. The first resonance is due to the fundamental mode $HEM_{11\delta}$ and the other two resonances due to the higher-order hybrid modes $HEM_{21\delta}$ and $HEM_{13\delta}$. The theoretical resonant frequency $HEM_{11\delta}$ for specified CDRA dimension is 4.97 GHz [11], and $HEM_{21\delta}$ is approximately estimated at 6.52 GHz [12]. A new higher-order mode $HEM_{13\delta}$ is obtained without any enlargement in antenna dimension with an aspect ratio (height/radius) ≈ 0.6 for the relative permittivity of CDRA ≈ 10. The non-resonant triangular slot in the ground plane with microstrip feed excites three hybrid modes, $HEM_{11\delta}$ at 4.36 GHz, $HEM_{21\delta}$ at 6.56 GHz, and $HEM_{13\delta}$ at 8.89 GHz in CDRA simultaneously with different radiation patterns. The parametric analysis (Figure 2) of S_{11} for different base lengths and heights of triangular slot has been done using CST Microwave studio simulation. The base length "b" and its distance from origin "c" were properly chosen for three resonance frequencies. The feed line length was varied to provide a better impedance match for all the resonance frequencies. The triangle was optimized to an equilateral triangle with the orientation shown in Figure 1 with $a = 6$, $b = 10.39$ mm, and $c = 3$ mm.

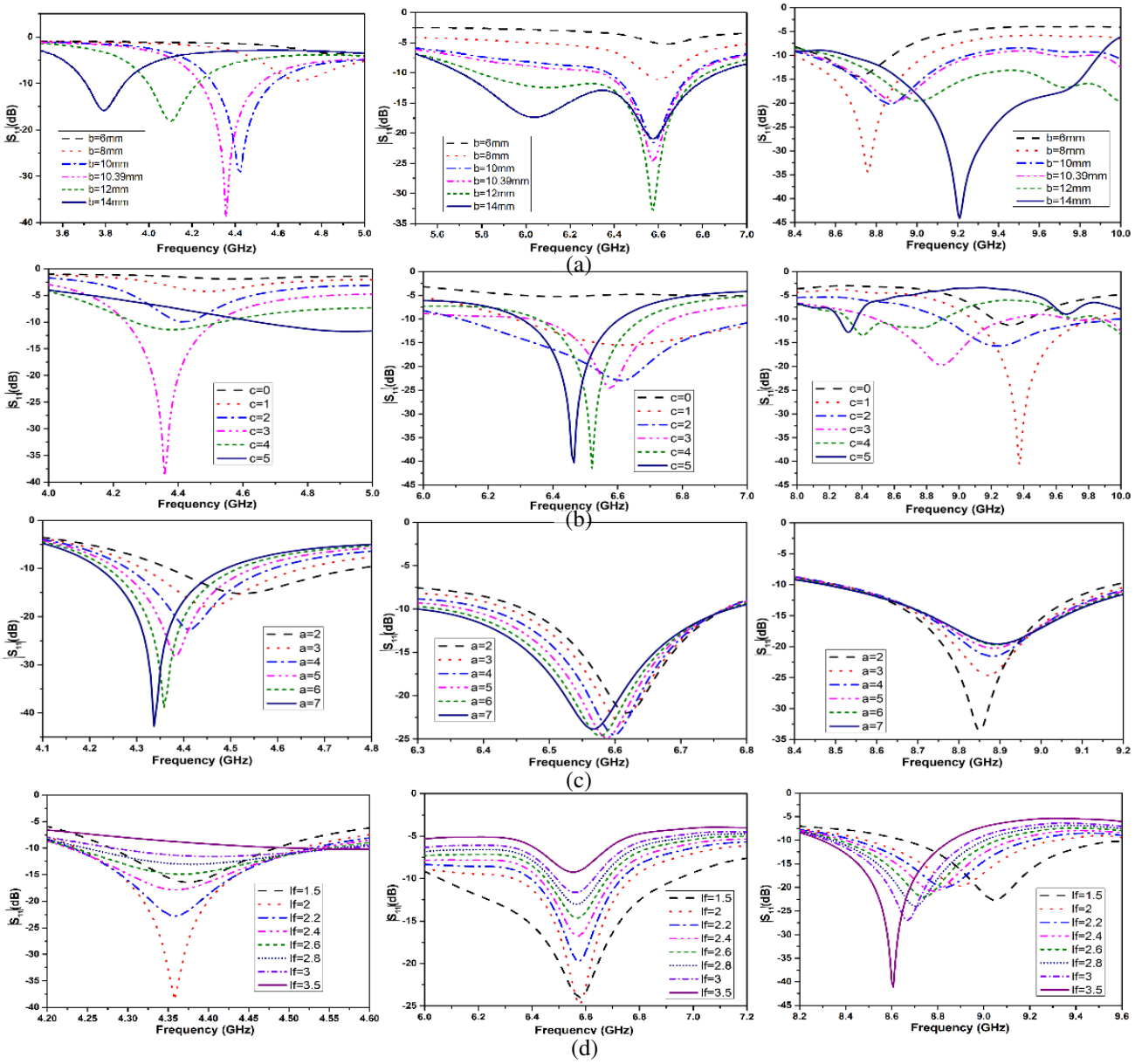

Figure 2. Reflection coefficient S_{11} variation of the proposed LP CDRA with respect to parameter (a) b, (b) c, (c) a and (d) l_f.

2.2. Simulation and Measurement Results

Figure 3 displays the contour and near field distribution at 4.36 GHz, 6.56 GHz, and 8.89 GHz. From the near field distribution at 4.36 GHz and 6.56 GHz, the modes are easily recognized as $HEM_{11\delta}$ and $HEM_{21\delta}$, respectively [13]. The third mode is identified as $HEM_{13\delta}$ mode and named using the nomenclature as in [13]. Figure 4 shows simulated and measured results of S_{11} of the proposed triband LP CDRA. The simulated impedance bandwidths ($S_{11} \leq -10$ dB) in the first, second, and third bands were 6.62% (4.23–4.52 GHz), 6.87% (6.32–6.77 GHz), and 9.55% (8.47–9.32 GHz), respectively, and measured impedance bandwidths were 4.38% (4.24–4.43 GHz), 6.81% (6.38–6.83 GHz), and 15.5% (8.26–9.65 GHz), respectively.

Simulated and measured gains of 5.7 dBi and 5.4 dBi at 4.4 GHz, 8.2 dBi, and 8 dBi were observed at 8.89 GHz, respectively. A high gain was observed at higher-order mode $HEM_{13\delta}$. The simulated and

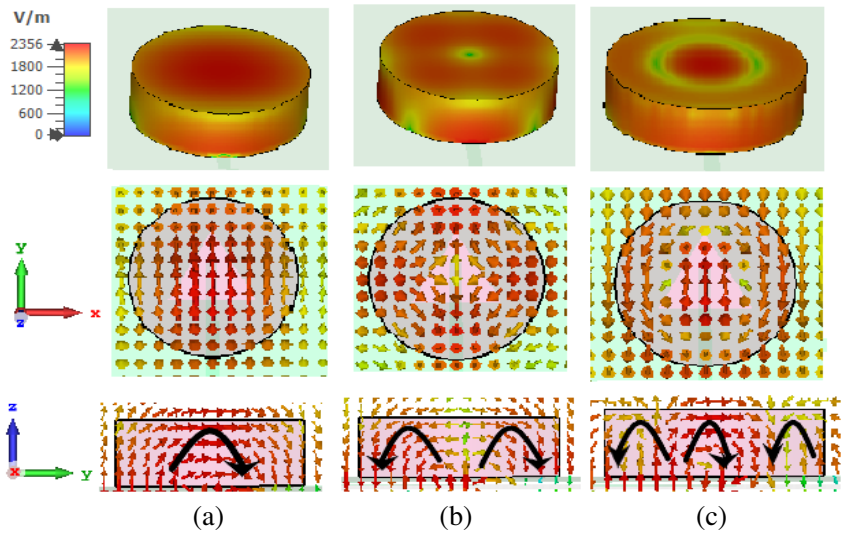

Figure 3. Contour and electric field distribution of the proposed triband LP CDRA in xy and yz plane at (a) 4.36 GHz, (b) 6.56 GHz, and (c) 8.89 GHz.

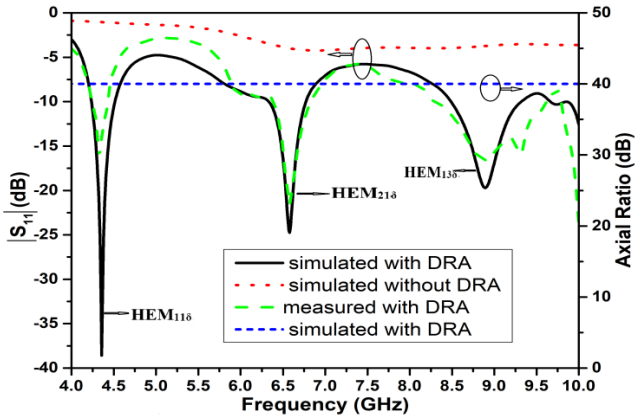

Figure 4. Simulated and measured results of S_{11} versus frequency of the proposed triband LP CDRA.

measured radiation patterns in the xz and yz planes are shown in Figure 5. At 4.3 GHz, $HEM_{11\delta}$ mode is excited which results in broadside radiation, and $HEM_{13\delta}$ is a higher mode of $HEM_{11\delta}$ which also results in broadside radiation. $HEM_{21\delta}$ results in quadrupole radiation. Due to unsymmetrical field distribution in the far-field region, a high gain was observed at theta = 36° with 3.9 dBi and 2 dBi at theta = 0°.

3. CIRCULARLY POLARIZED CYLINDRICAL DIELECTRIC RESONATOR ANTENNA

In this section, the triband LP CDRA is used to provide circularly polarized bands with modified feed without changing the DR geometry and triangular aperture slot. The flag shape microstrip feed generates additional hybrid radiating modes $HEM_{21\delta\text{-like}}$, $HEM_{12\delta}$, and $HEM_{14\delta}$ resulting in six different modes. Three CP bands are obtained in the third impedance band. Figure 6 shows the top view of the antenna with different layers and a fabricated prototype of the top and bottom layers of the substrate. The weak coupling modes ($HEM_{12\delta}$ and $HEM_{14\delta}$) of triband LP CDRA are made to resonate. The modification of the feed has enhanced the S_{11} bandwidth and changed the AR response.

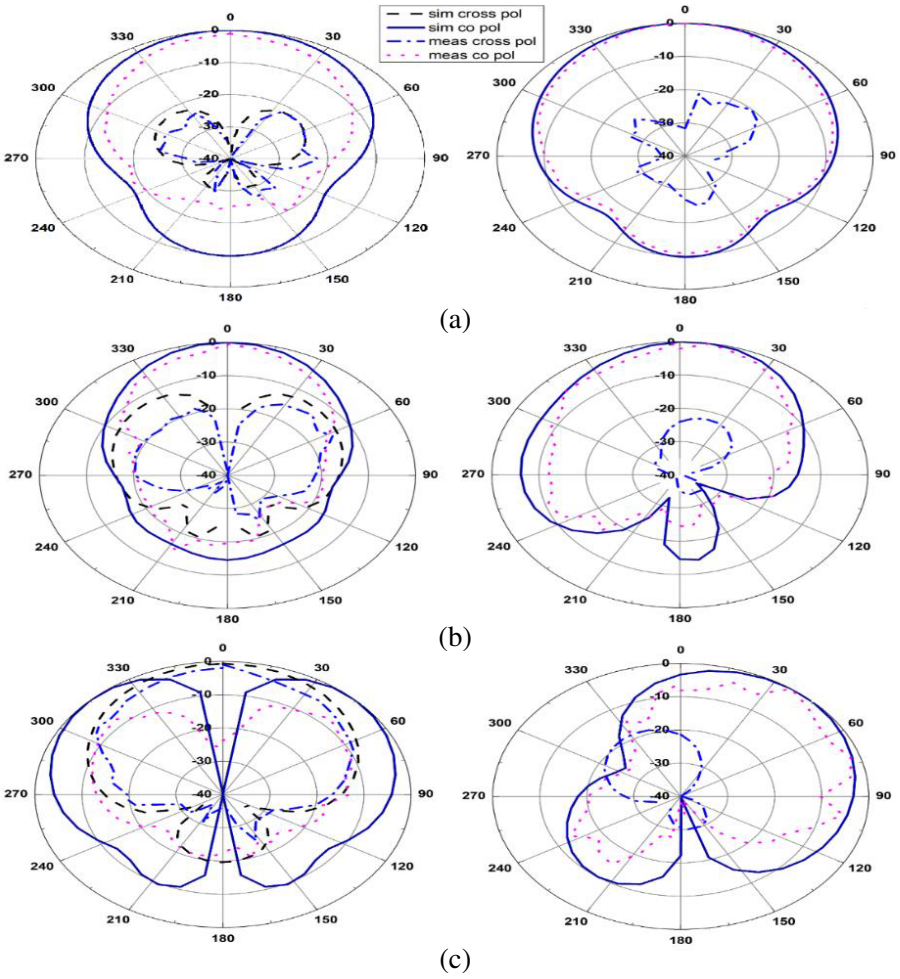

Figure 5. Simulated and measured results of normalized radiation patterns of the proposed triband LP CDRA at (a) 4.4 GHz, (b) 8.8 GHz and (c) 6.5 GHz in the xz and yz plane.

3.1. CP Waves Creation

It is a well-known fact that CP waves are created by the same amplitude orthogonal component of an E-field. Default hybrid modes are degenerative modes. The hybrid modes are divided into HE and EH modes. HE_{m+1n} and EH_{m-1n} modes generally degenerate. The coupling between the EH and HE modes changes their polarization state and field configuration.

3.2. Results and Discussion

The proposed CP CDRA was fabricated to validate the simulated results. The parameters p, q, s, l_f, and w_{ss} were optimized to obtain the triband CP band. The near field electric distribution was used to identify the hybrid radiating mode of $HEM_{11\delta}$, $HEM_{21\delta\text{-like}}$, $HEM_{21\delta}$, $HEM_{12\delta}$, $HEM_{13\delta}$, and $HEM_{14\delta}$, generated at 4.68 GHz, 6.23 GHz, 6.66 GHz, 8.45 GHz, 9.12 GHz, and 9.74 GHz. The electric field distributions of $HEM_{12\delta}$ and $HEM_{14\delta}$ are shown in Figure 7. Figure 8(a) shows simulated and measured results of S_{11}. An additional resonance frequency was observed at 6.23 GHz which is the slot resonance. The verified theoretical resonance frequency of the triangular slot is 6.14 GHz [14]. The simulated first band is 4.38–4.99 GHz (13.02%), the second band 5.95–7.12 GHz (17.90%), and the third band 8.05–9.79 GHz (19.51%). The measured impedance bands were 4.23–4.53 GHz (6.84%), 5.95–6.91 GHz (14.93%), and 7.69–9.95 GHz (25.62%), respectively. A high gain was obtained in the third impedance

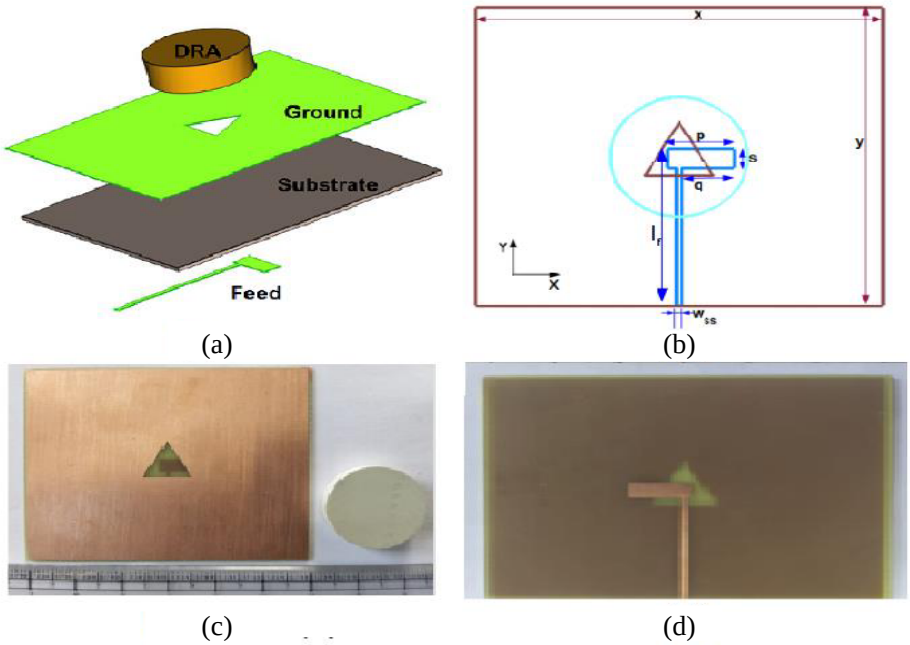

Figure 6. (a) 3D view of different layers of the proposed CP CDRA, (b) top view of the proposed CP CDRA with all the layers. Fabricated prototype of the proposed CP CDRA, (c) triangular slot on the ground plane and (d) bottom view of the substrate. $x = 60$, $y = 50$, $r = 10$, $w_{ss} = 1.2$, $l_f = 31.48$, $p = 9.8$, $q = 8$ and $s = 3.48$ (all dimensions are in mm).

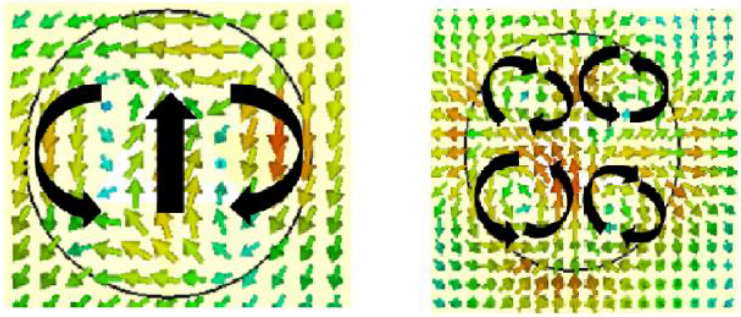

Figure 7. Electric field distribution in the xy plane at (a) 8.45 GHz and (b) 9.74 GHz.

band. The simulated and measured gains at 4.7 GHz and 8.7 GHz were 5.7 dBic, 5.6 dBic, 7.5 dBic, and 7 dBic, respectively at $\phi = 0°$ and $\theta = 0°$. At 6.5 GHz radiation beam is tilted due to $HEM_{21\delta}$ mode, and the maximum simulated gain of 5 dBic is obtained at $\theta = 36°$.

Figure 8(b) shows simulated and measured results of axial ratio (AR) response. The measured 3 dB AR bandwidths in the third impedance band were 8.53–8.64 GHz (1.28%), 9.05–9.15 GHz (1.09%), and 9.48–9.56 GHz (0.84%), and simulated values were 8.52–8.64 GHz (1.39%), 9.03–9.14 GHz (1.21%), and 9.15–9.54 GHz (0.315%). One more CP at 4.3 GHz with $S_{11} \approx -9$ dB was observed with an AR bandwidth of 4.34–4.38 GHz. Since the value of S_{11} is not less than -10 dB, the result is not presented here. Further analysis can be done to achieve CP bands in the first and second impedance bands. The simulated electric field distribution is analyzed at different resonance frequencies in the $+z$ direction in the xy plane of the proposed CP CDRA. The clockwise rotation of E-field is observed at 8.6 GHz and 9.5 GHz. Hence, right-hand circular polarization (RHCP) is obtained. The anticlockwise rotation of the E-field is observed at 9.1 GHz, indicating left-hand circular polarization (LHCP). The far-field of the

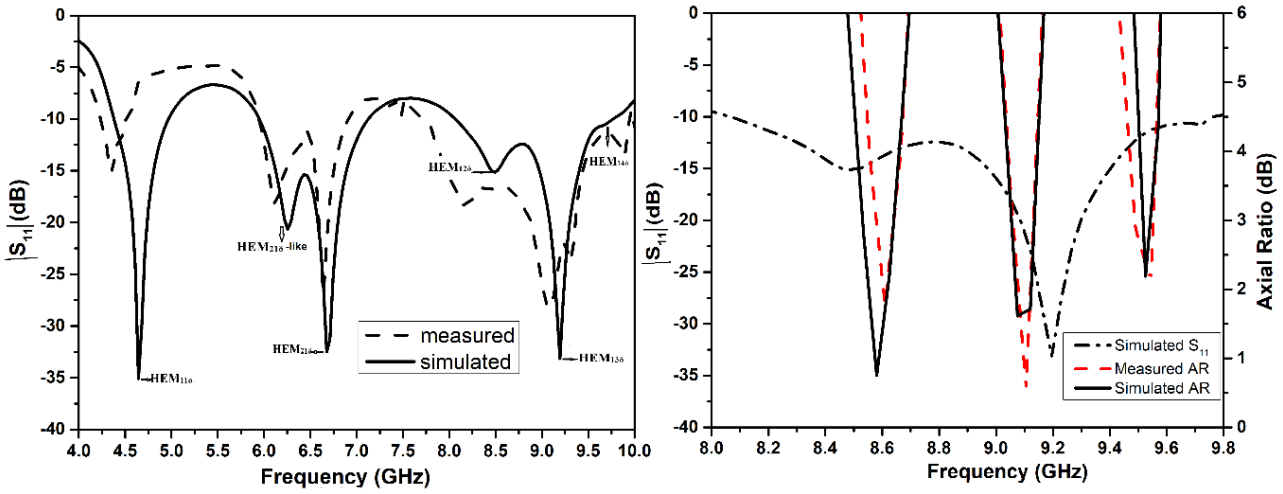

Figure 8. Simulated and measured results of the proposed CP CDRA. (a) S_{11} and (b) axial ratio.

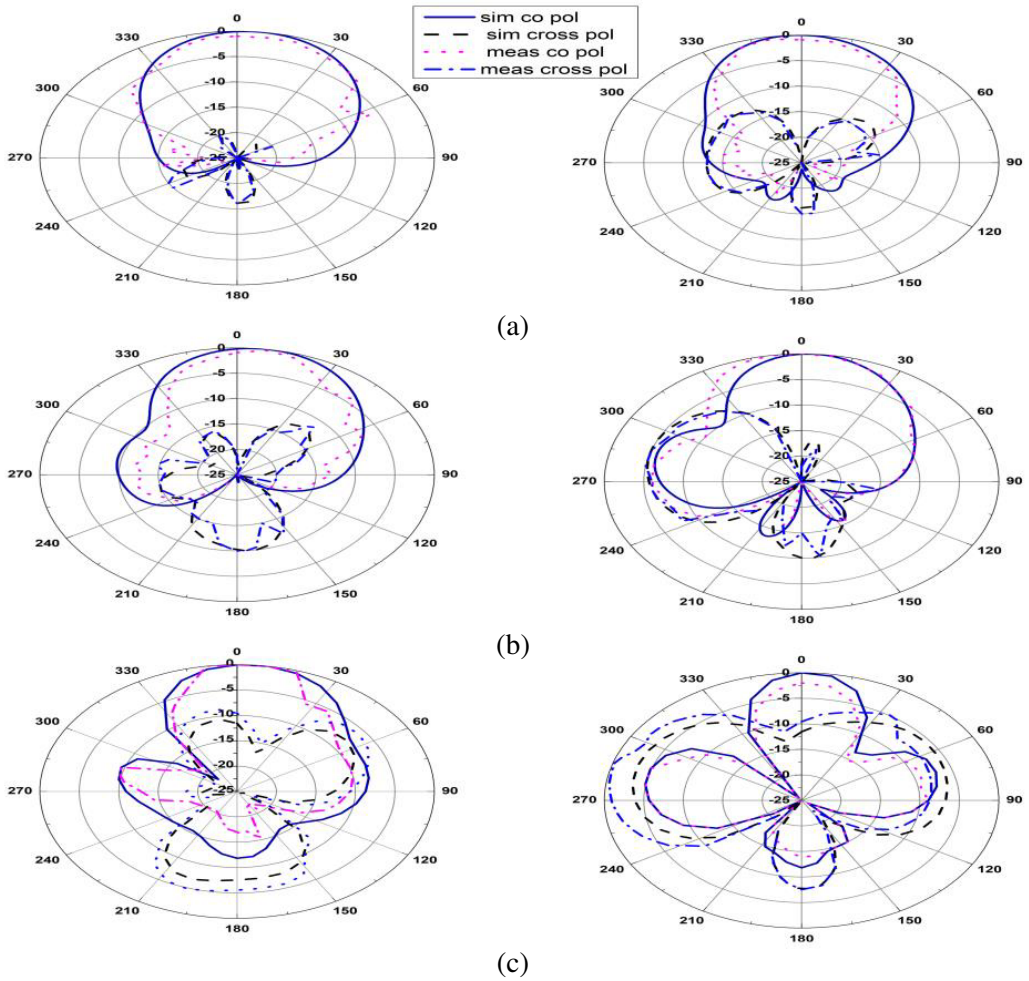

Figure 9. Simulated and measured results of normalized radiation patterns of the proposed CP CDRA in the xz and yz plane at (a) 8.6 GHz, (b) 9.1 GHz and (c) 9.5 GHz.

Table 1. Comparison of present work with earlier reported work (DRA $\epsilon_r \approx 10$).

Feed configuration	DRA Vol (mm^3)	Modes	F_o (GHz)	Impedance Bandwidth GHz	Peak Gain (dBi)	CP bandwidth (%)
Cross-shaped composite aperture [4]	3142	$HEM_{11\delta}$	3.9	7%	5.6	-
		$HEM_{12\delta}$	7.4	8%	6	
Twin aperture [6]	3142	$HEM_{11\delta}$	3.85	10%	6.3	-
		$HEM_{111+\delta}$	7.85	10%	9	
Triangular aperture [Present LP CDRA]	1995	$HEM_{11\delta}$	4.36	4.38%	5.7	-
		$HEM_{21\delta}$	6.56	6.81%	3.9	
		$HEM_{13\delta}$	8.89	15.5%	8.2	
Strategic shaped aperture with cross-shaped microstrip feed [5]	127000	$HEM_{11\delta}$	1.1	0.97–1.2 (0.23 GHz)	5	11.65
		$HEM_{111+\delta}$	1.57	1.46–1.66 (0.2 GHz)		7.64
		($HEM_{12\delta\text{-like}}$ +$HEM_{12\delta}$ +$HEM_{13\delta}$)	2.28	1.89–2.48 (0.59 GHz)		7.01
		$HEM_{14\delta}$	2.6	2.55–2.75 (0.2 GHz)		7.1
Inverted pentagon-shaped with quarter annular stub loaded feed-line [16]	6902	$HEM_{11\delta}$	2.6	2.58–2.96 (0.38 GHz)	5.5	-
		($HEM_{11\delta}$ +$HEM_{12\delta}$)	5.5	4.83–5.93 (1.1 GHz)	6.2	8.78
Triangular aperture with flag-shaped microstrip feedline. [Present CP CDRA]	1995	$HEM_{11\delta}$	4.68	4.23–4.53 (0.3 GHz)	5.7	1.28 1.09 0.84
		($HEM_{21\delta\text{-like}}$ +$HEM_{21\delta}$)	6.5	5.95–6.91 (0.96 GHz)	5	
		($HEM_{12\delta}$ +$HEM_{13\delta}$ +$HEM_{14\delta}$)	9.12	7.65–9.95 (2.3 GHz)	7.5	

CP CDRA was obtained using a single horn antenna [15]. Figure 9 shows the measured and simulated radiation patterns in the boresight direction at the CP band frequencies. A good separation between LHCP and RHCP fields is observed in both the *xz* and *yz* planes. Table 1 provides the comparison between the existing literature and the proposed CDRA.

4. CONCLUSION

A triband hybrid radiating LP CDRA and a CP CDRA are presented. The hybrid modes are achieved using a novel triangular aperture slot. A new $HEM_{13\delta}$ mode is excited with a simple aperture without suppressing fundamental mode $HEM_{11\delta}$ and weak mode $HEM_{21\delta}$. The circular polarization is obtained using a flag-shaped feed and triangular slot. The proposed antennas are easy to fabricate with a basic cylindrical dielectric resonator and simple aperture feed.

REFERENCES

1. Guha, D., A. Banerjee, C. Kumar, and Y. M. Antar, "Higher-order mode excitation for high-gain broadside radiation from cylindrical dielectric resonator antennas," *IEEE Transactions on Antennas and Propagation*, Vol. 60, No. 1, 71–77, 2011.

2. Guha, D., A. Banerjee, C. Kumar, and Y. M. M. Antar, "New technique to excite higher-order radiating mode in a cylindrical dielectric resonator antenna," *IEEE Antennas and Wireless Propagation Letters*, Vol. 13, 15–18, 2014.
3. Sharma, A., P. Ranjan, and R. K. Gangwar, "Multiband cylindrical dielectric resonator antenna for WLAN/WiMAX application," *Electronics Letters*, Vol. 53, No. 3, 132–134, 2016.
4. Guha, D., P. Gupta, and C. Kumar, "Dual band cylindrical dielectric resonator antenna employing $HEM_{11\delta}$ and $HEM_{12\delta}$ modes excited by new composite aperture," *IEEE Transactions on Antennas and Propagation*, Vol. 63, No. 1, 433–438, 2015.
5. Sharma, A., G. Das, S. Gupta, and R. K. Gangwar, "Quadband quad-sense circularly polarized dielectric resonator antenna for GPS/CNSS/WLAN/WiMAX applications," *IEEE Antennas and Wireless Propagation Letters*, Vol. 19, No. 3, 403–407, 2020.
6. Gupta, P., D. Guha, and C. Kumar, "Dual-mode cylindrical DRA: Simplified design with improved radiation and bandwidth," *IEEE Antennas and Wireless Propagation Letters*, 2021.
7. Sharma, A., G. Das, P. Ranjan, N. K. Sahu, and R. K. Gangwar, "Novel feeding mechanism to stimulate triple radiating modes in cylindrical dielectric resonator antenna," *IEEE Access*, Vol. 4, 9987–9992, 2016.
8. Zhou, Y.-D., Y.-C. Jiao, Z.-B. Weng, and T. Ni, "A novel single-fedwide dual-band circularly polarized dielectric resonator antenna," *IEEE Antennas and Wireless Propagation Letters*, Vol. 15, 930–933, 2015.
9. Fang, X., K. W. Leung, and E. H. Lim, "Singly-fed dual-band circularly polarized dielectric resonator antenna," *IEEE Antennas and Wireless Propagation Letters*, Vol. 13, 995–998, 2014.
10. Varshney, G., S. Gotra, V. Pandey, and R. Yaduvanshi, "Inverted-sigmoid shaped multiband dielectric resonator antenna with dual-band circular polarization," *IEEE Transactions on Antennas and Propagation*, Vol. 66, No. 4, 2067–2072, 2018.
11. Petosa, A., *Dielectric Resonator Antenna Handbook*, Artech House Publishers, 2007.
12. Guha, D., H. Gajera, and C. Kumar, "Cross-polarized radiation in a cylindrical dielectric resonator antenna: Identification of source, experimental proof, and its suppression," *IEEE Transactions on Antennas and Propagation*, Vol. 63, No. 4, 1863–1867, 2015.
13. Kajfez, D., A. W. Glisson, and J. James, "Computed modal field distributions for isolated dielectric resonators," *IEEE Transactions on Microwave Theory and Techniques*, Vol. 32, No. 12, 1609–1616, 1984.
14. Garg, R., P. Bhartia, I. J. Bahl, and A. Ittipiboon, *Microstrip Antenna Design Handbook*, Artech House, 2001.
15. Wang, D., M. Wang, N. Xu, and W. Wu, "Improved measurement method of circularly-polarized antennas based on linear-component amplitudes," *Open Journal of Antennas and Propagation*, Vol. 5, No. 1, 36–45, 2017.
16. Sharma, A., G. Das, and R. K. Gangwar, "Dual-band dual-polarized hybrid aperture-cylindrical dielectric resonator antenna for wireless applications," *International Journal of RF and Microwave Computer-Aided Engineering*, Vol. 27, No. 5, e21092, 2017.